4 PRELIMINARY ANALYSIS

4.1 VIBRATORY RIGS

As it can be seen from Tables 12 and 13, as well as Figs 12 ÷ 18 different design features and operating parameters result in different erosion rates. In most cases cavitation resistance of materials rises in the sequence of their appearance in the tables although significant differences in the $MDPR_{max}$ ratios can be easily stated. However, in case of the CISE rig the carbon steel 45 appears to show higher resistance than the 1H18N9T chromium nickel steel and the M63 brass shows higher resistance than the E04 Armco iron. One reason for such a performance can be seen in high intensity of cavitation which results in lack of work-hardening effect (typical for 1H18N9T steel) and plastic deformations prevailing over the fatigue erosion mechanism. Similar inversion between the steels tested can be observed at the Cape Town stationary specimen rig.

A peculiar feature of the erosion curves obtained at vibrating specimen rig in Tsinghua University is relatively high damage rate of the 45 carbon steel (Figs.13, 14). A suspicion exists that this might be due to testing an improper material. Another peculiarity is extremely high volume loss of tarnamide specimens tested in Beijing. Non-uniform mechanical properties of this material cannot be excluded.

Erosion curves determined at the Hull University lab (Figs.16, 17) are very symptomatic for stationary specimen rigs. After a period of intense erosion (comparable with that at the University of Cape Town), the volume loss rate of M63 brass, E04 Armco iron and 45 carbon steel falls dramatically to the value close to zero. The effect can be explained by rising distance between the vibrating horn and the sample in course of erosion progress which results in removing the exposed surface out of the highly localised space of erosive impingement. Due to this special feature, the *CER* (cumulative erosion rate) and *CEPR* (cumulative erosion penetration rate) parameters describe much better erosion curves determined at the Hull University lab than the *IER* and *MDPR* parameters[1].

Results obtained in Hull prove also the essential significance of exposed surface processing. In case of soft materials (PA2, M63, E04) the damage of specimens with previously polished surface was even several times smaller than that of other ones.

Mean depth of erosion penetration curves resulting from brass, Armco iron, carbon steel and chromium nickel steel tests at different vibrating specimen vibratory rigs (Fig 15) confirm the amplitude effect although in case of the IMP PAN rig vibration frequency seems to be of essential significance and in case of the Hiroshima University rig, the temperature effect should not be disregarded.

A general correlation between *p-p* vibration amplitude and the $MDPR_{max}$ can be derived for vibrating specimen rigs although a significant scatter of data exists. The last remark refers especially to the results from the Tsinghua University. The *MDP* values attained here are one order of magnitude smaller then the corresponding values at other rigs of the same vibration frequency and even higher vibration amplitudes.

[1] In most other cases the maximum *CER* value was not attained.

Table 12a Test Series Summarisation Table of the CISE vibrating specimen vibratory rig (f = 20 kHz, $A_{p\text{-}p}$ = 50 μm)

material	*test duration*	*volume loss*	*eroded area*[1]	*incubation period*	$MDPR_{max}$
	min	mm^3	mm^2	min	μm/min
PA2	360	128.96	174.27	6	6.100
M63	600	107.18	174.27	8	1.420
E04	600	123.73	174.27	30	1.830
45	1200	61.97	174.27	67	0.385
1H18N9T	1200	79.55	174.27	33	0.450

Table 12b Test Series Summarisation Table of the CSSRC vibrating specimen vibratory rig (f = 20 kHz, $A_{p\text{-}p}$ = 32 μm)

material	*test duration*	*volume loss*	*eroded area*	*incubation period*	$MDPR_{max}$
	min	mm^3	mm^2	min	μm/min
PA2	150	15.15	174.1	4.4	0.980
M63	210	8.48	107.4	34.0	0.450
E04	310	4.07	107.0	61.0	0.192
45	440	4.65	129.7	108.0	0.118
1H18N9T	600	2.51	135.0	88.0	0.043

Table 12c Test Series Summarisation Table of the HIRO vibrating specimen vibratory rig (f = 19.9 kHz, $A_{p\text{-}p}$ = 24 μm)

material	*test duration*	*volume loss*	*eroded area*	*incubation period*	$MDPR_{max}$
	min	mm^3	mm^2	min	μm/min
PA2	120	16.17	163.0	1.5	1.530
M63	360	19.56	163.0	250	0.448
E04	360	18.08	163.0	56	0.489
45	1140	14.33	163.0	100	0.102
1H18N9T	2100	7.25	163.0	800	0.037

[1] impinged surface area

Table 12d Test Series Summarisation Table
of the IMP vibrating specimen vibratory rig (f = 8.1 kHz, $A_{p\text{-}p}$ = 50 μm)

material	*test duration*	*volume loss*	*eroded area*	*incubation period*	$MDPR_{max}$
	min	mm^3	mm^2	min	μm/min
PA2	360	45.448	122.7	13	1.730
M63	360	18.172	122.7	30	0.570
E04	360	15.092	122.7	30	0.480
45	360	10.798	122.7	44	0.380
1H18N9T	360	4.196	122.7	109	0.132
tarnamide	360	2.871	122.7	28	0.073

Table 12e Test Series Summarisation Table
of the TSING vibrating specimen vibratory rig (f = 19.8 kHz, $A_{p\text{-}p}$ = 35 μm)

material	*test duration*	*volume loss*	*eroded area*[1]	*incubation period*	$MDPR_{max}$
	min	mm^3	mm^2	min	μm/min
PA2	50	3.268	294.5	1.5	0.650
M63	50	0.427	294.5	8.5	0.064
E04	150	0.372	294.5	29.0	0.023
45	150	0.456	294.5	3.7	0.021
1H18N9T	480	0.435	294.5	57.0	0.0046
tarnamide	70	6.663	294.5	1.6	1.58

Table 12f Test Series Summarisation Table
of the VSB vibrating specimen vibratory rig (f = 20 kHz, $A_{p\text{-}p}$ = 40 μm)

material	*test duration*	*volume loss*	*eroded area*	*incubation period*	$MDPR_{max}$
	min	mm^3	mm^2	min	μm/min
M63	140	5.03	131	48	0.440
E04	300	4.86	105	69	0.216
45	540	5.74	132	115	0.102
1H18N9T	600	2.09	75	82	0.066

[1] impinged surface area

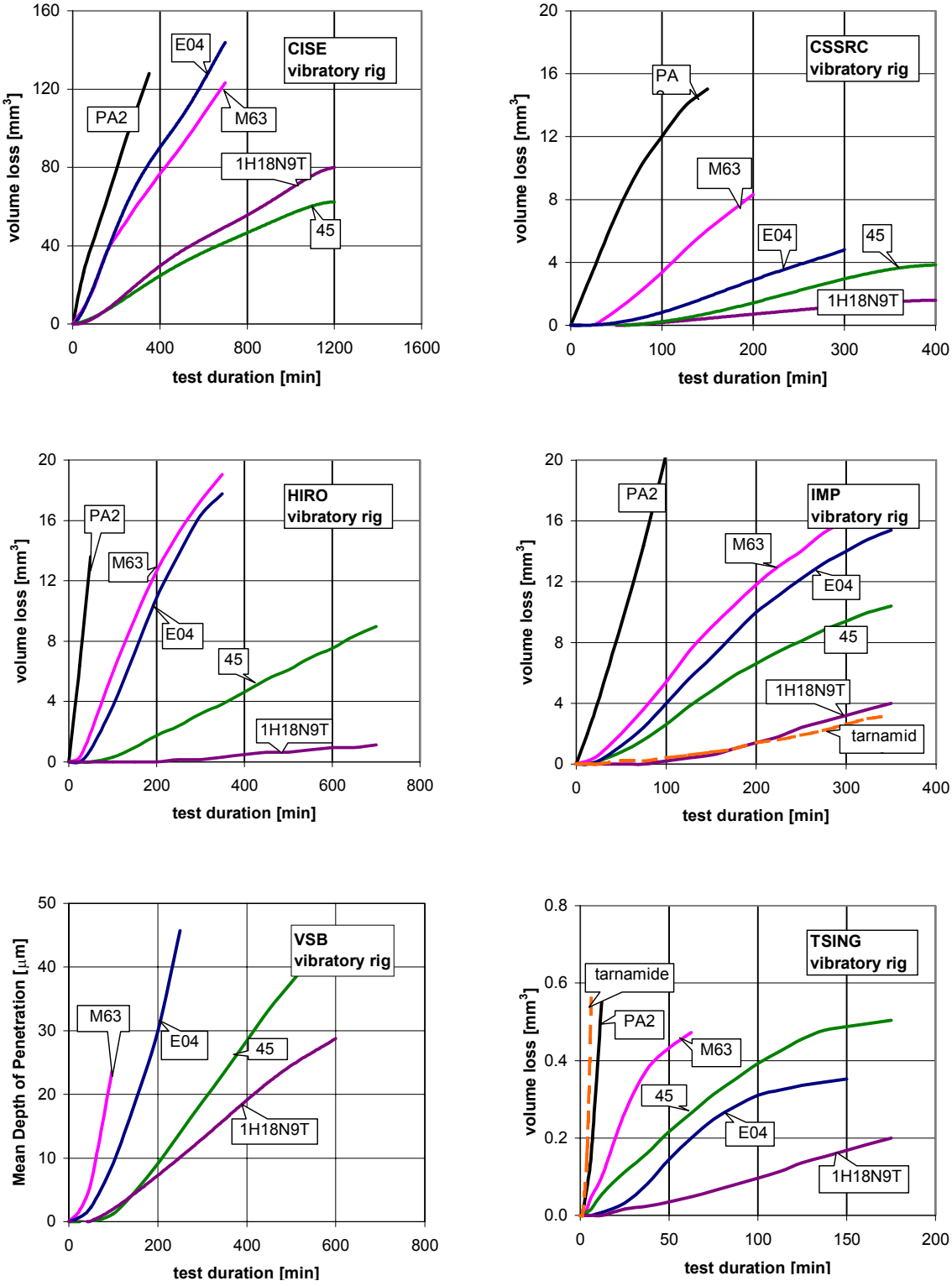

Fig.13 Cumulative volume loss curves of the ICET materials tested at the vibrating specimen vibratory rigs

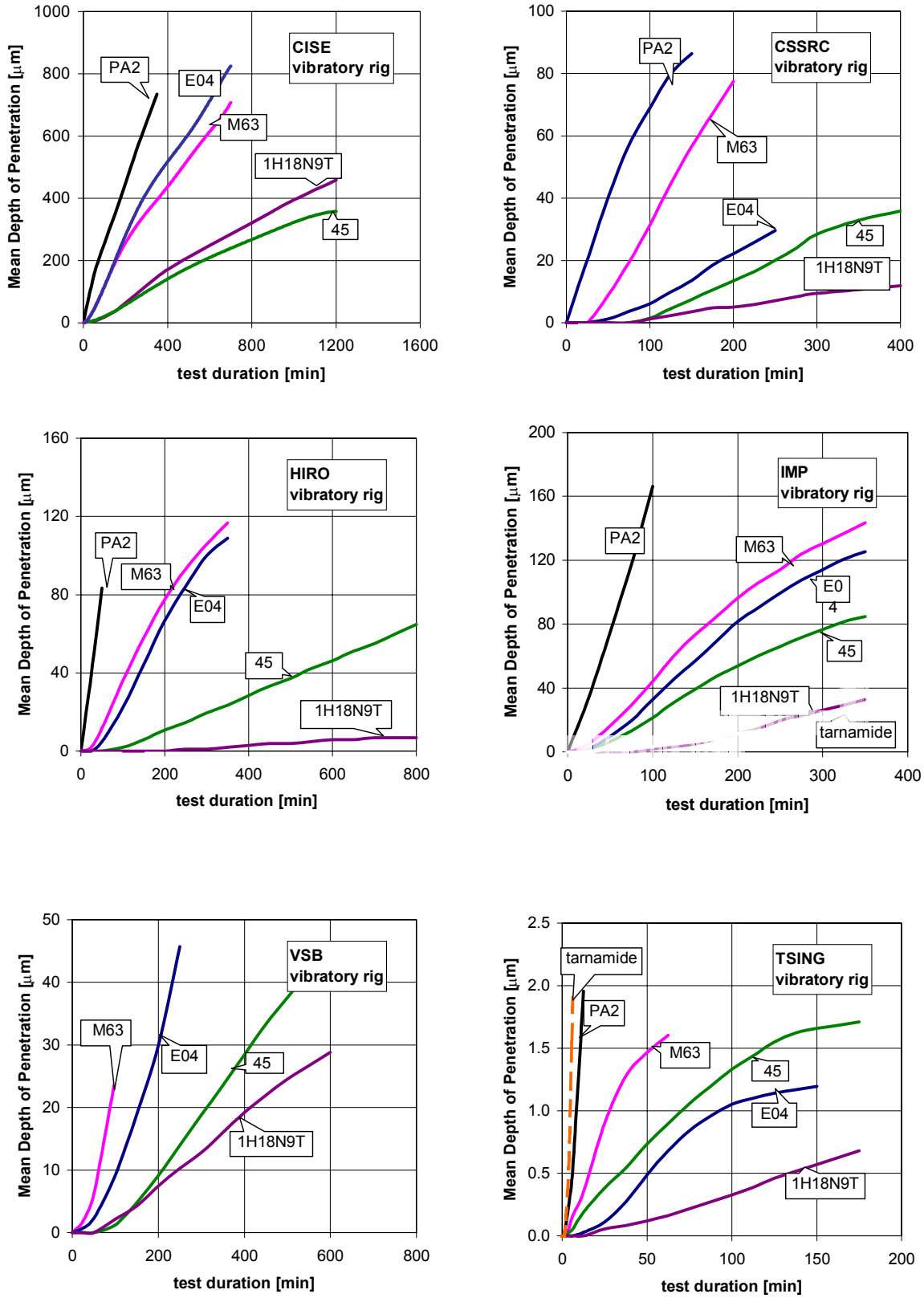

Fig.14 Mean depth of erosion penetration curves of the ICET materials tested at the vibrating specimen vibratory rigs

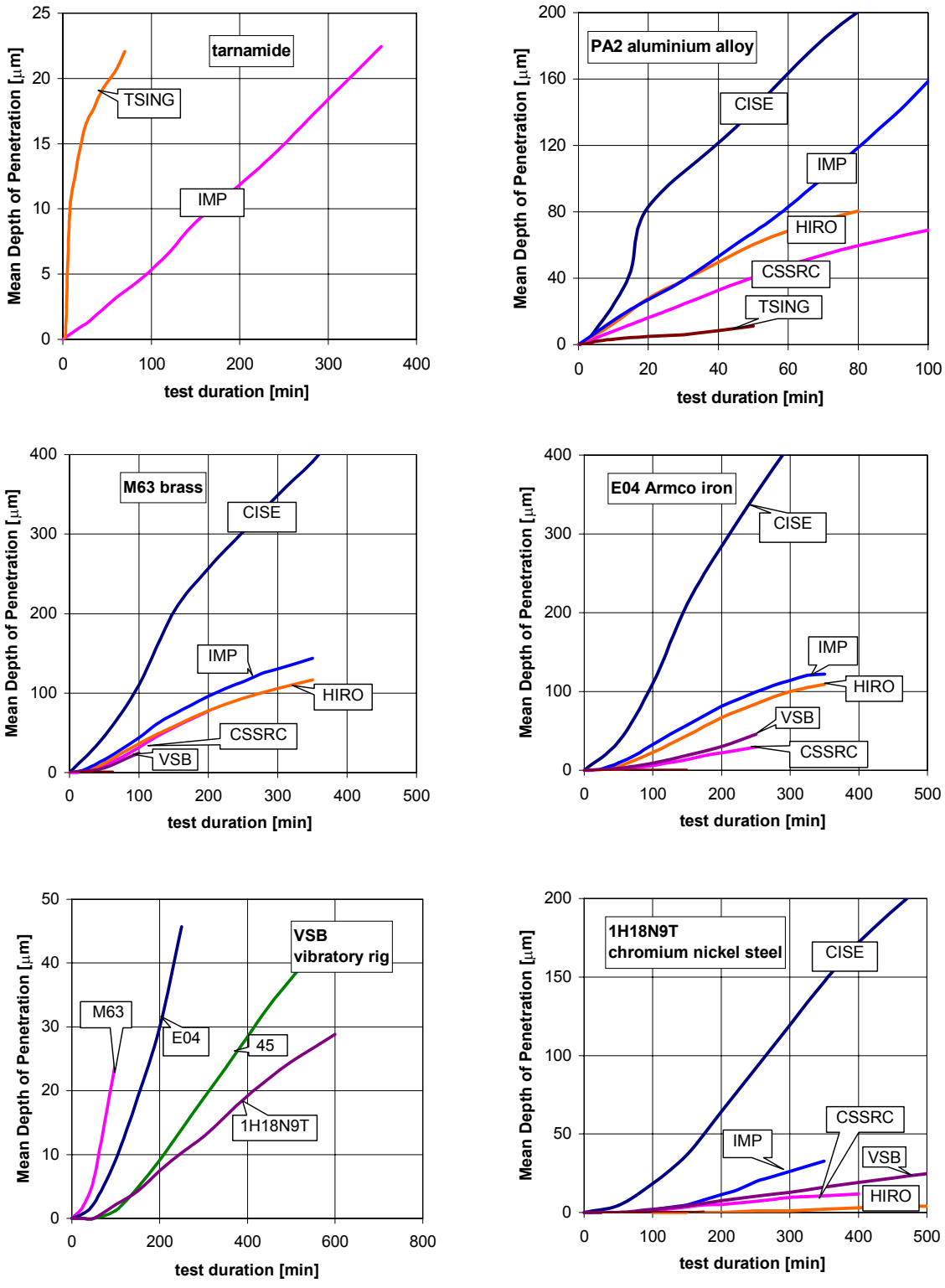

Fig.15 Mean depth of erosion penetration curves of the ICET materials tested at the vibrating specimen vibratory rigs

Table 13a Test Series Summarisation Table
of the CAP stationary specimen vibratory rig (f = 20 kHz, $A_{p\text{-}p}$ = 60 μm, δ = 0.35 mm)

material	*test duration*	*volume loss*	*eroded area*	*incubation period*	$MDPR_{max}$
	min	mm^3	mm^2	min	μm/min
PA2	360	89.31	91.6	8	6.9
M63	360	14.44	77.65	38	0.56
E04	360	10.82	70.25	85	0.56
45	360	3.26	69.32	85	0.17
1H18N9T	360	3.94	71.56	72	0.19
tarnamide	1320	6.32	71.87	0	0.21

Table 13b Test Series Summarisation Table
of the HIRO stationary specimen vibratory rig (f = 20 kHz, $A_{p\text{-}p}$ = 28 μm, δ = 0.4 mm)

material	*test duration*	*volume loss*	*eroded area*	*incubation period*	$MDPR_{max}$
	min	mm^3	mm^2	min	μm/min
PA2	150	31.67	170	29	1.675
M63	1230	37.11	170	67	0.206
E04	1260	40.44	170	250	0.230
45	4680	31.83	170	333	0.046
1H18N9T	6060	5.76	170	530	0.007

Table 13b Test Series Summarisation Table
of the HULL stationary specimen vibratory rig (f = 20 kHz, $A_{p\text{-}p}$ = 117 μm, δ = 0.5 mm)

material	*test duration*	*volume loss*	*eroded area*	*incubation period*	$MDPR_{max}$
	min	mm^3	mm^2	min	μm/min
PA2	720	75.8	211.3	9	4.76
M63	720	17.95	131.3	44	0.60
E04	720	9.4	129.2	73	0.69
1H18N9T	720	4.4	123.9	40	0.09

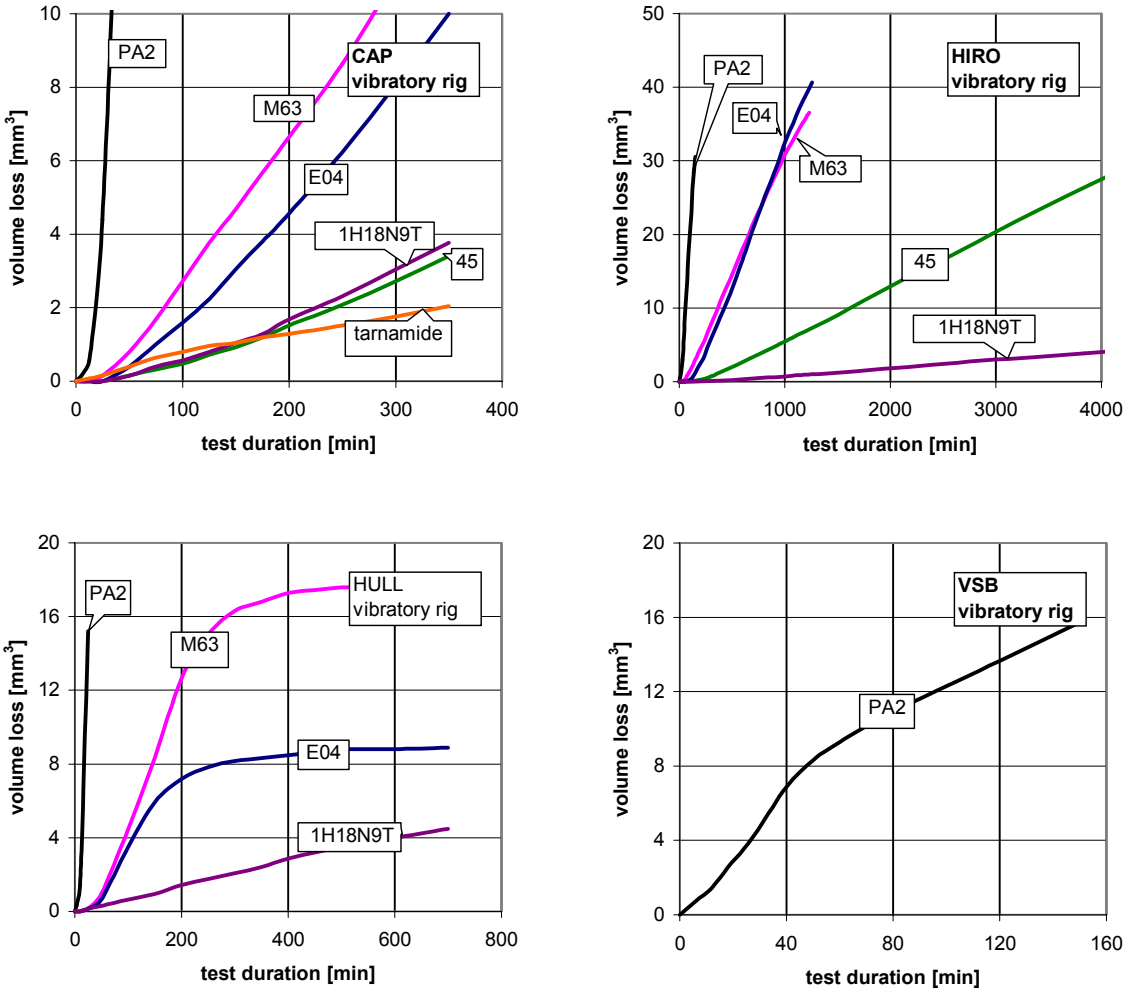

Fig.16 Cumulative volume loss curves of the ICET materials tested at the stationary specimen vibratory rigs

Apart from the Tsinghua results, the amplitude effect is much more significant than that of frequency. This is especially the case for the 45 carbon steel which is characterised by substantial hardness and very high yield strength. It can be seen from Fig.15 that the results of CISE and IMP coincide throughout a major part of the erosion acceleration period despite very significant difference in vibration frequencies. One may suppose that while high vibration frequency accelerates the rise and collapse of cavities, lower frequency gives more time for rectified diffusion and allows for larger cavity sizes and higher values of cavity collapse energy.

In case of stationary specimen rigs one can see from Fig.18 that applying lower horn/specimen distance may allow for shorter exposures with relatively high erosion rates.

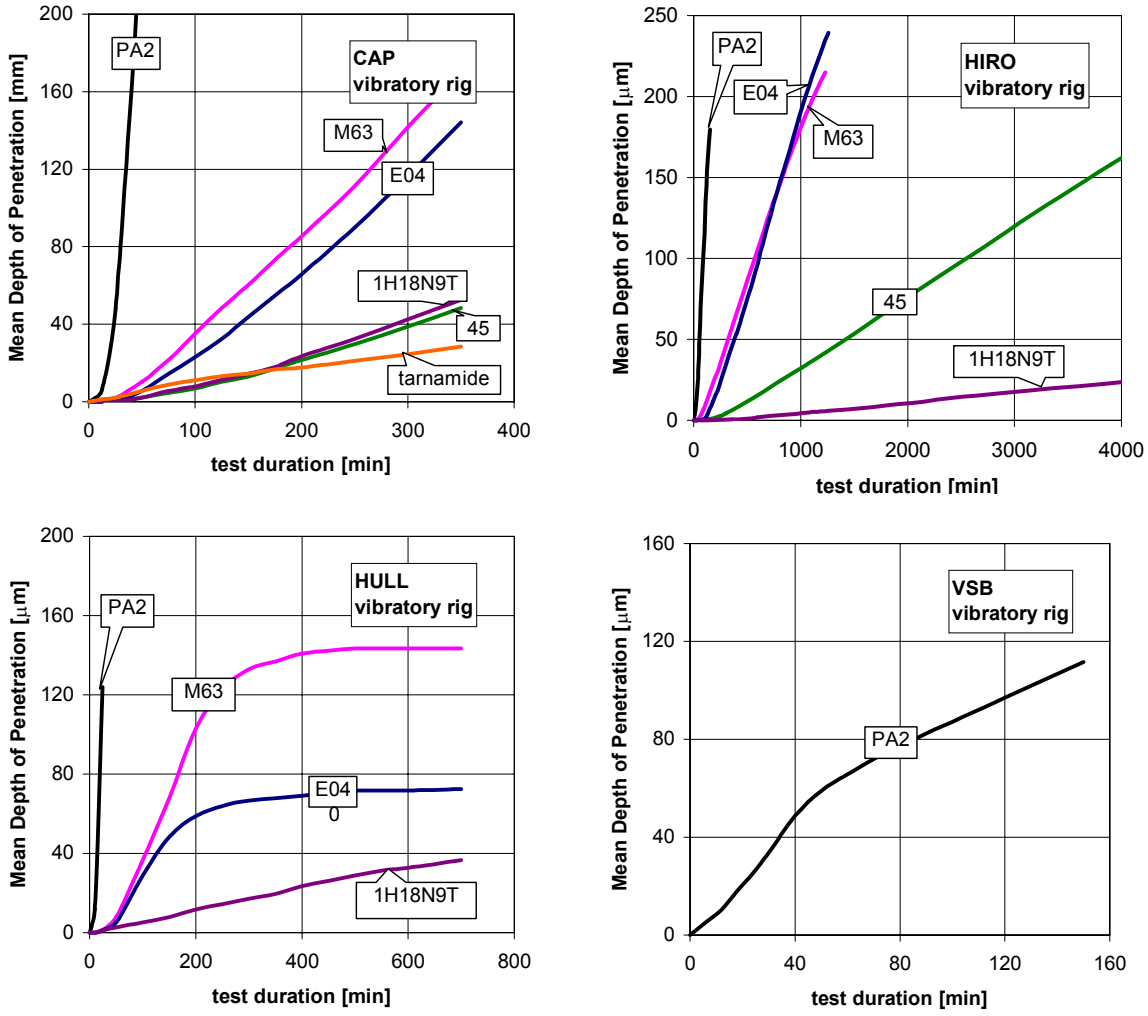

Fig.17 Mean depth of erosion penetration curves of the ICET materials tested at the stationary specimen vibratory rigs

Differentiation of results between various facilities usually depends on the material tested. By comparing *MDP* curves of two reference materials tested at vibrating specimen rigs (Fig.15) one can easily notice that PA2 specimens show smaller differentiation of damage than the E04 ones. In fact it is only in case of PA2 test that the erosion curve determined in Beijing could be plotted using the same volume loss scale as for the curves determined by other labs. The highest differentiation can be stated in case of the 1H18N9T chromium nickel steel which is often subject to significant work hardening.

In case of stationary specimen rigs (Fig.18),differentiation of results for aluminium, Armco iron, brass and carbon steel is of the same order. Substantial rise is observed for the 1H18N9T steel.

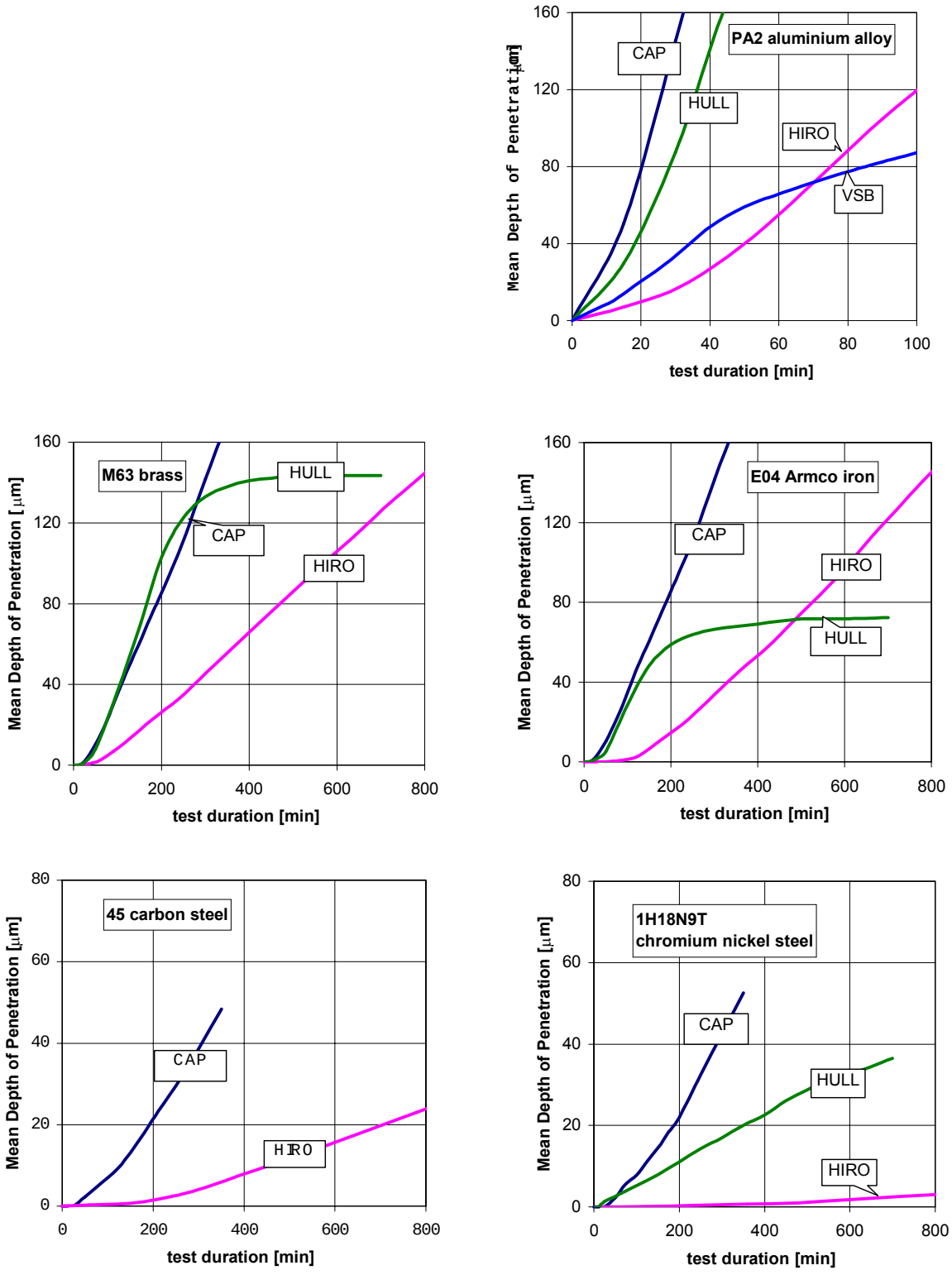

Fig.18 Mean depth of erosion penetration curves of the ICET materials tested at the stationary specimen vibratory rigs